

Electronic Supplementary Information for:

A Rare Example of a Phosphine as a Halogen Bond Acceptor

Yijue Xu,[‡] Jasmine Huang,[‡] Bulat Gabidullin,[‡] and David L. Bryce^{‡,*}

[‡]Department of Chemistry and Biomolecular Sciences
University of Ottawa
10 Marie Curie Private
Ottawa, Ontario K1N 6N5
Canada

*Author to whom correspondence is to be addressed
Tel: +1-613-562-5800 ext.2018; fax: +613-562-5170
Email: dbryce@uottawa.ca

EXPERIMENTAL

Sample Preparation

Triphenylphosphine (Ph_3P) was purchased from Sigma Aldrich and 1,3,5-trifluoro-2,4,6-triiodobenzene (*sym*- $\text{C}_6\text{F}_3\text{I}_3$) was purchased from Alfa Aesar. Both starting materials were used without any further purification. Equimolar amounts of these two starting materials were dissolved into a minimum volume of diethyl ether, chloroform, or acetonitrile. Slow evaporation from diethyl ether or chloroform at room temperature produced crystals of **1**, along with a trace amount of **2**. Slow evaporation from acetonitrile at room temperature produced a crystal of **2**. Single cocrystals of **1** and **2** were individually wrapped in aluminum foil and stored in the freezer. Storage at room temperature or under light for more than two days caused the cocrystals to start decomposing and change from colourless to yellow.

The mechanochemical preparation of **1** was carried out using a Retsch MM 400 ball mill. 0.0872 g Ph_3P and 0.1663 g *sym*- $\text{C}_6\text{F}_3\text{I}_3$ were added with 50 μL acetonitrile to 10 mL stainless steel milling jars. The mixture was milled for 30 min at room temperature with a milling frequency of 30 Hz using two 5 mm stainless steel grinding balls.

Equimolar amounts of Ph_3P (0.1020 g) and *sym*- $\text{C}_6\text{F}_3\text{I}_3$ (0.2005 g) were first dissolved in a minimum of nearly boiling diethyl ether. The mixture was left in the freezer overnight. The precipitation of cocrystal **1** was effected by filtering under vacuum. The phase purity of compounds obtained from each method was verified by powder X-ray diffraction (see Figures S2 and S3).

³¹P Solution NMR Spectroscopy

³¹P NMR spectra were recorded in CDCl₃ using a 300 MHz Bruker Avance II spectrometer. A sealed capillary tube containing 85% H₃PO₄ was inserted into the 5 mm o.d. NMR tube in each experiment to serve as an internal reference. ³¹P NMR chemical shifts were referenced to 85% H₃PO₄ in H₂O (δ = 0 ppm).

³¹P Solid-State NMR Spectroscopy

Data were acquired with a 9.4 T magnet, Bruker AVANCE III console, and a 4 mm Bruker HXY probe (University of Ottawa, Ottawa, Canada). Samples were packed into 4 mm o.d. zirconia rotors. ³¹P chemical shifts were referenced to ammonium dihydrogen phosphate (δ_{iso} = 0.81 ppm with respect to 85% H₃PO₄). A standard cross-polarization pulse sequence was employed. The $\pi/2$ pulse length and contact time were 3.5 μ s and 3 ms, respectively. The recycle delay was set to be 4 minutes and the number of scans was 16 for Ph₃P. The recycle delay was set to be 2 min for the cocrystals and the number of scans was 312 for **1** and 576 for **2**. Data were acquired for Ph₃P under static and MAS conditions. Data for cocrystal **1** were acquired at different magnetic fields (4.7 T and 9.4 T) to identify the isotropic peak and to obtain spectra with a larger number of sidebands for spectral fitting purposes.

Powder X-ray Diffraction

All PXRD patterns were obtained using a Rigaku Ultima IV powder diffractometer at room temperature (298 \pm 1 K) with a copper source and one diffracted beam monochromator from 5° to 50° (2 θ range) in increments of 0.02° with a scan rate of 1° per minute. Simulations were generated using Mercury 3.8 software from the Crystallographic Data Center. Comparisons between experimental PXRD patterns and simulated patterns were used to verify sample phase purity.

Computational Details

For DFT calculations on cluster models, electrostatic potential calculations were performed using B3LYP.¹ The calculation for Ph₃P was carried out using the 6-311++G(d,p) basis set. The Def2TZVP basis set was used for *sym*-C₆F₃I₃ and co-crystal **1** which contain the heavy atom iodine. Models were constructed and visualized using GaussView 4.1 software.²

Single-crystal X-ray diffraction

The crystal of **1** and **2** were mounted on a thin glass fiber using paraffin oil. Prior to data collection the crystal was cooled to 200 ± 2 K. Data was collected on Bruker AXS single crystal diffractometer equipped with a sealed Mo tube source (wavelength 0.71073 Å) and APEX II CCD detector. Raw data collection and processing were performed with Bruker APEX II software package.³ Semi-empirical absorption corrections based on equivalent reflections were applied.⁴ The structure was solved by direct methods and refined with a full-matrix least-squares procedure based on F^2 , using SHELXL⁵ and WinGX⁶. All non-hydrogen atoms were refined anisotropically. The positions of hydrogen atoms were calculated based on the geometry of related non-hydrogen atoms. No additional restraints or constraints were applied during the refinement.

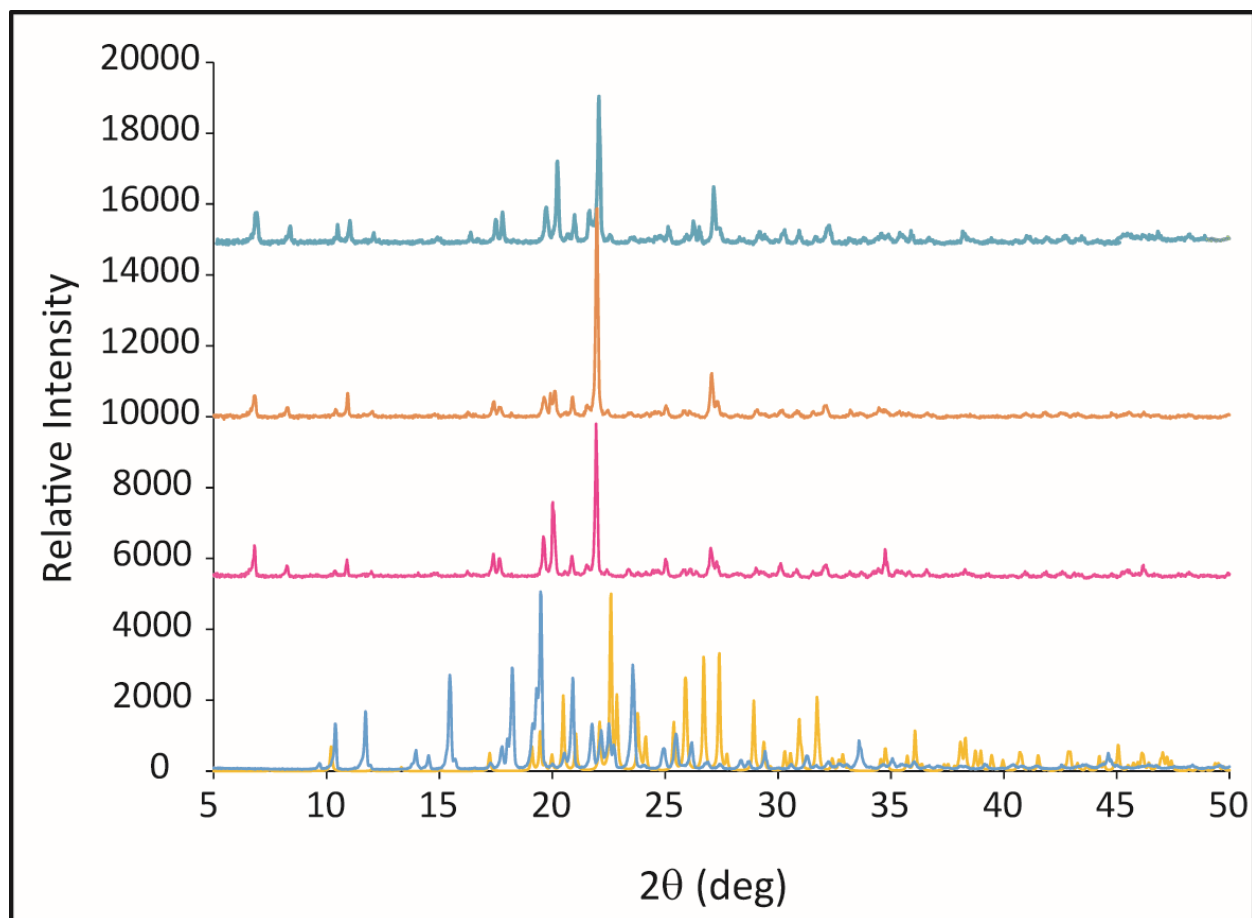


Figure S1. Experimental powder X-ray diffraction patterns for Ph_3P (blue), $\text{sym-C}_6\text{F}_3\text{I}_3$ (yellow) and halogen-bonded cocrystal **1** obtained by slow evaporation from diethyl ether at room temperature with different molar ratios of Ph_3P to $\text{sym-C}_6\text{F}_3\text{I}_3$: 2 (pink), 1 (orange) and 0.5 (dark green). All data were acquired using a Rigaku Ultima IV diffractometer with 2θ ranging from 5° to 50° at a rate of 1° per minute. The PXRD results indicate that different molar ratios of the starting materials always produced the same cocrystal.

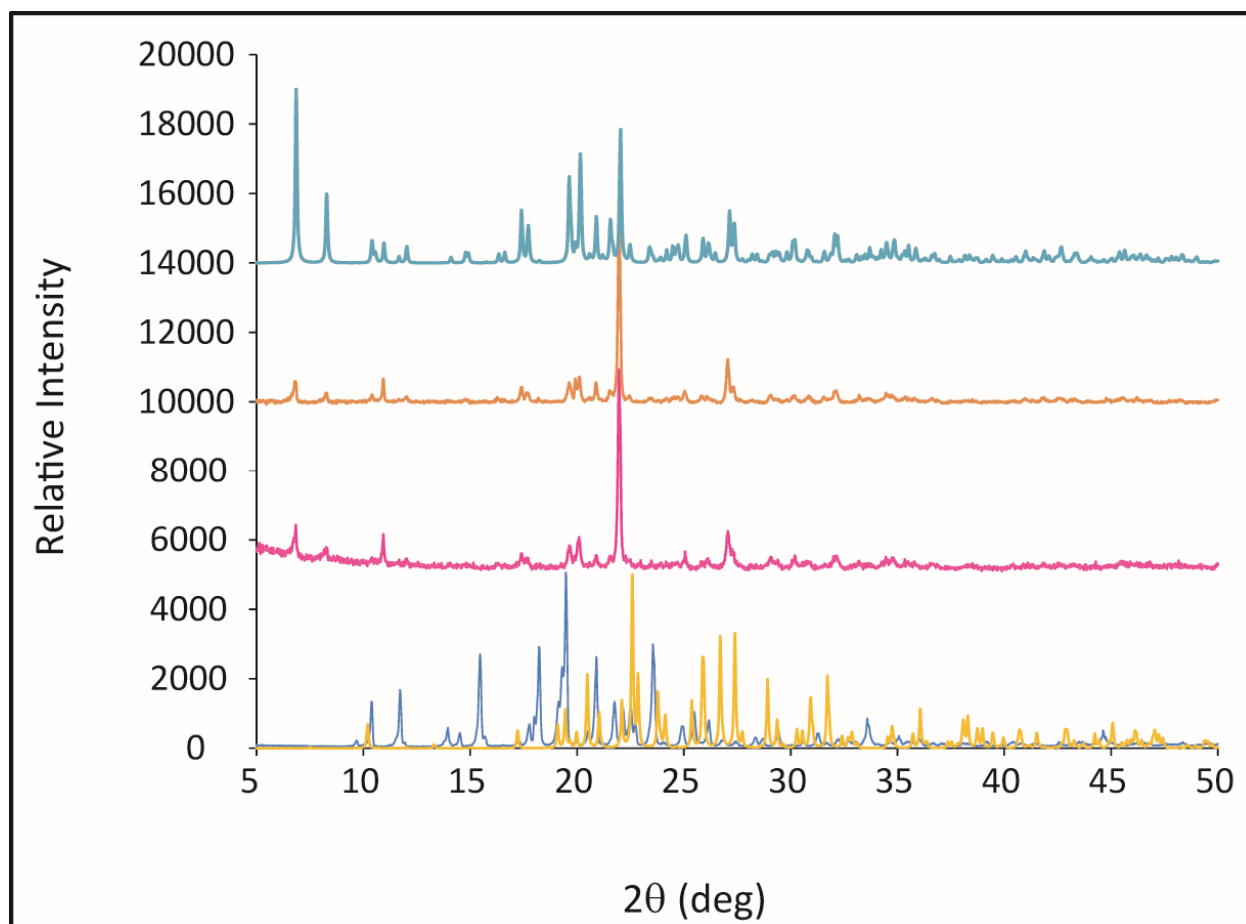


Figure S2. Experimental powder X-ray diffraction patterns for Ph_3P (blue), $\text{sym-C}_6\text{F}_3\text{I}_3$ (yellow) and halogen-bonded cocrystal **1** obtained by slow evaporation from different solvents at room temperature: chloroform (pink) and diethyl ether (orange). All data were acquired using a Rigaku Ultima IV diffractometer with 2θ ranging from 5° to 50° at a rate of 1° per minute. The simulated PXRD pattern from SCXRD structure generated by Mercury 3.10.2 is shown in dark green at top.

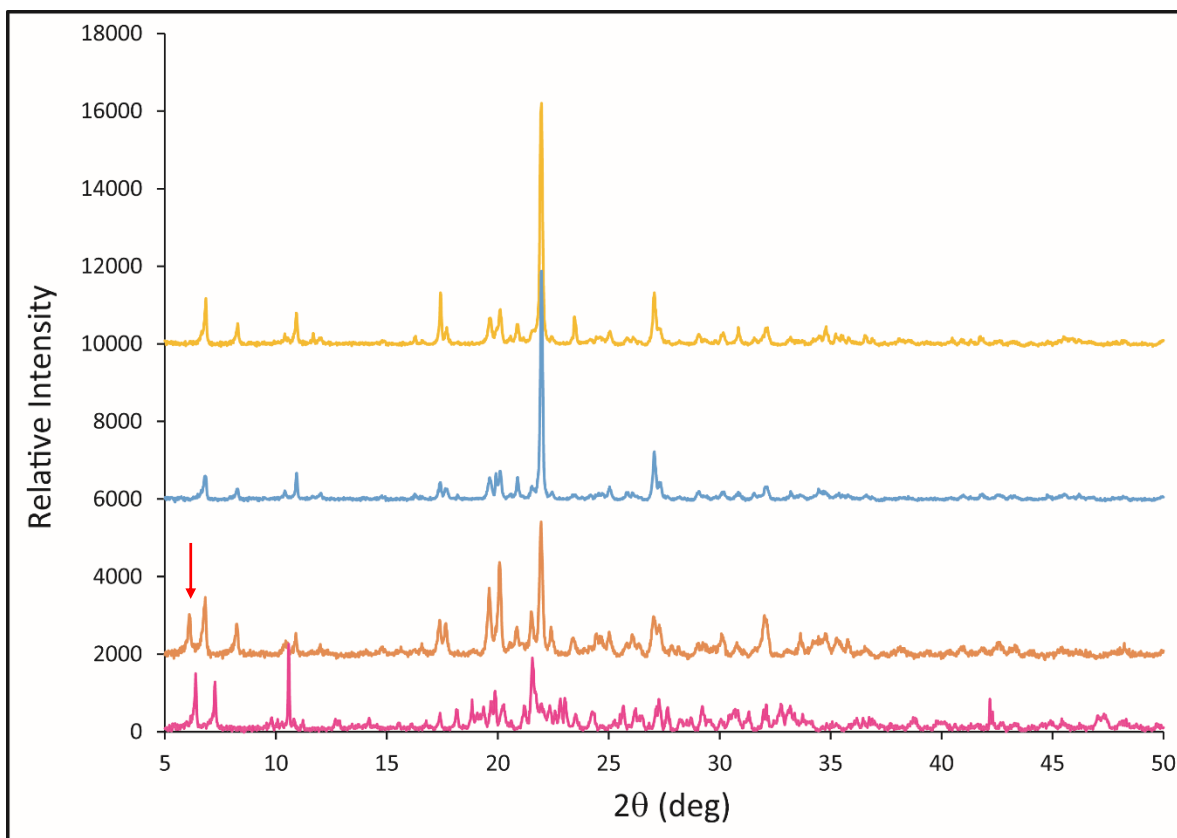


Figure S3. Experimental powder X-ray diffraction pattern for halogen-bonded cocrystal **1** obtained from different methods: ball milling with 50 μL acetonitrile (orange), cooling down a saturated diethyl ether solution (blue), and slow evaporation from diethyl ether at room temperature (yellow). All data were acquired using a Rigaku Ultima IV diffractometer with 2θ ranging from 5° to 50° at a rate of 1° per minute. The red arrow represents an impurity, which could be due to cocrystal **2** (shown in pink) or due to another impurity.

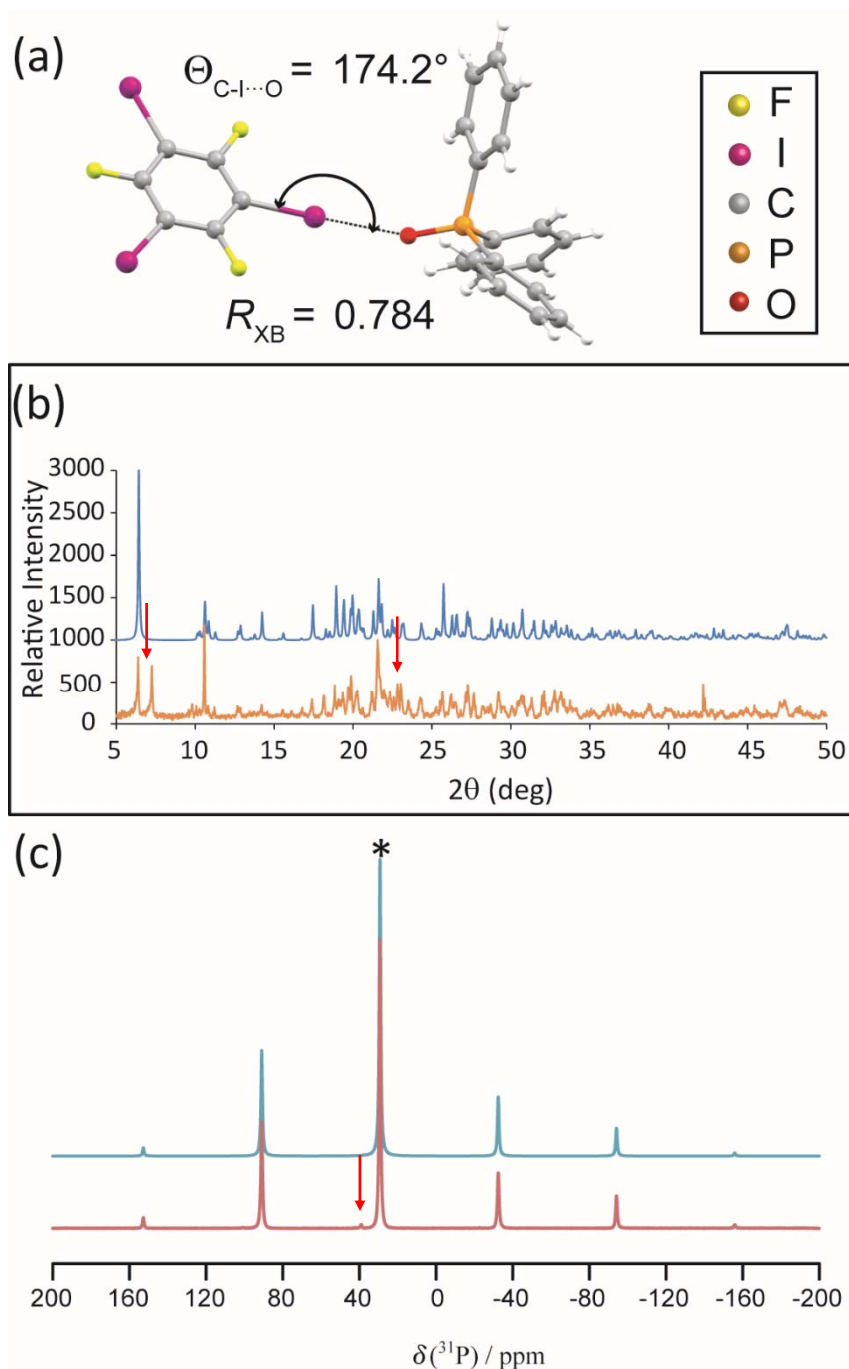


Figure S4. (a) Intermolecular geometry for halogen-bonded cocrystal **2** obtained from single-crystal X-ray diffraction. (b) Experimental (orange) and simulated (blue) powder X-ray diffraction patterns for the cocrystal **2** obtained from slow evaporation of acetonitrile at room temperature. All data were acquired using a Rigaku Ultima IV diffractometer with 2θ ranging from 5° to 50° at a rate of 1° per minute. Simulations were generated using Mercury 3.10.2 software. (c) Experimental (pink) and simulated (dark green) ^{31}P CP/MAS SSNMR spectra obtained at 9.4 T for the cocrystal **2** with MAS spinning speed of 10 kHz. The arrows in the PXRD and SSNMR spectra indicate a decomposition product.

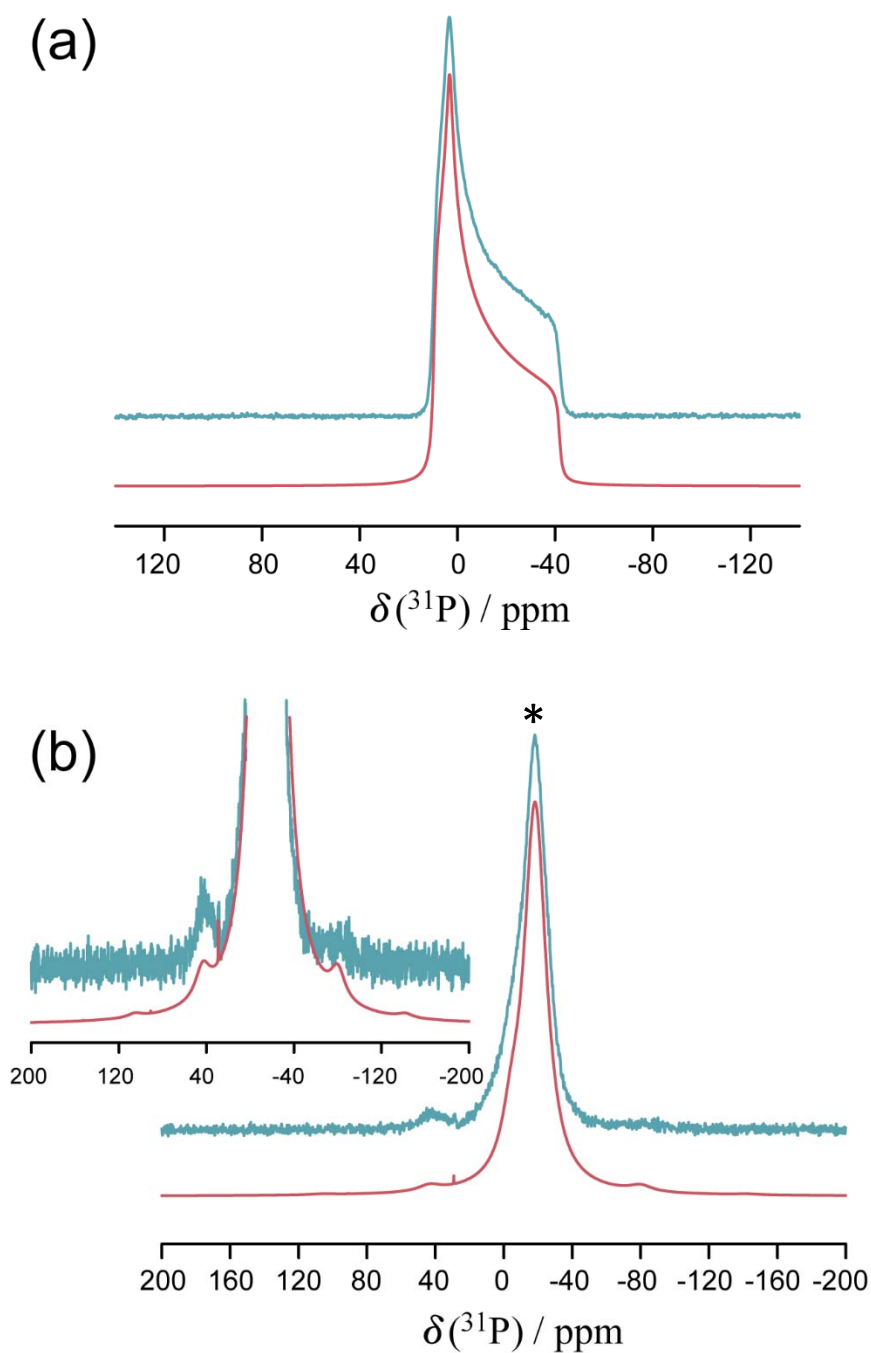


Figure S5. (a) Experimental static ^{31}P CP SSNMR spectra (dark green) obtained at 9.4 T for Ph_3P . (b) Experimental ^{31}P CP/MAS SSNMR spectra (dark green) obtained at 4.7 T for halogen-bonded cocrystal **1** with a spinning speed of 5 kHz. The isotropic peaks are indicated by asterisks. The corresponding simulated spectra are shown in pink. Shown in the inset is a magnified region of the spectrum.

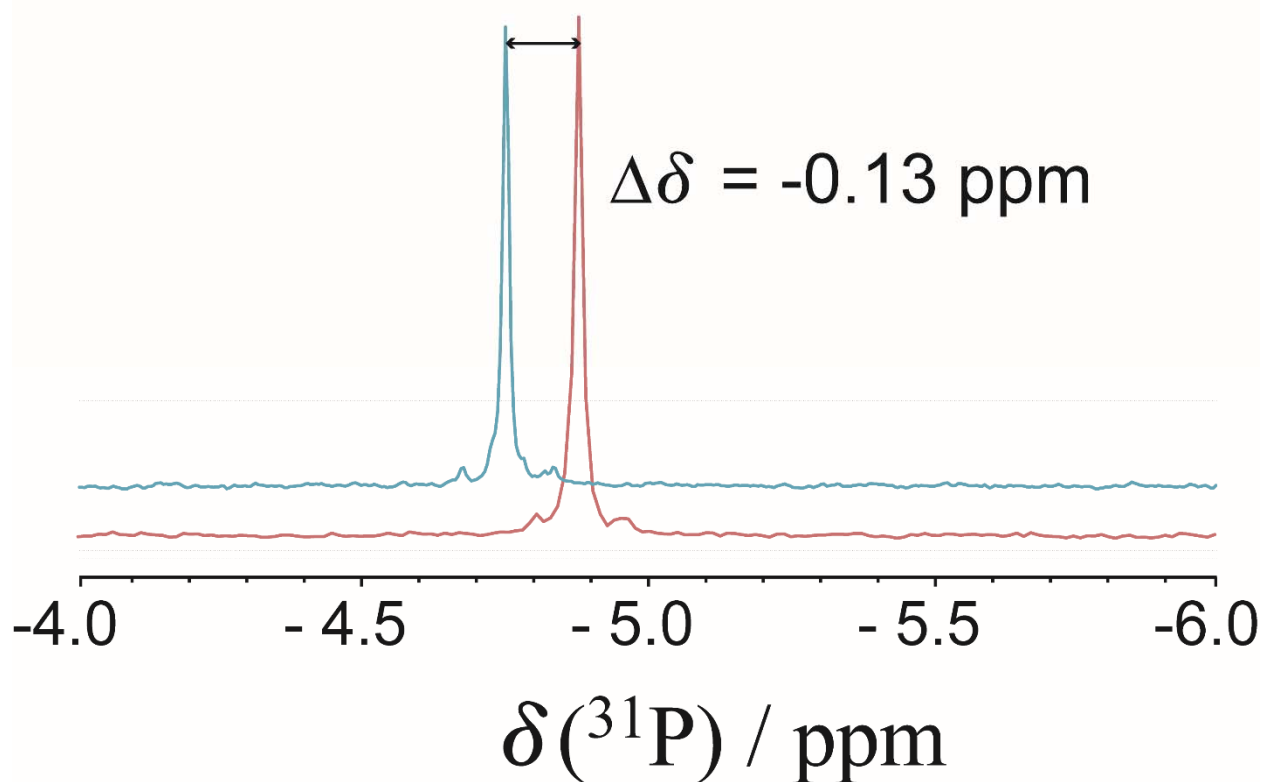


Figure S6. Experimental solution ^{31}P NMR spectra of Ph_3P (blue-green) and **1** (red) obtained at 7.05 T. The compounds were dissolved in CDCl_3 and referenced to 85% H_3PO_4 ($\delta = 0 \text{ ppm}$). There is a shielding of $\Delta\delta = -0.13 \text{ ppm}$ between Ph_3P ($\delta = -4.75 \text{ ppm}$) and a solution containing equimolar quantities of Ph_3P and *sym*- $\text{C}_6\text{F}_3\text{I}_3$ ($\delta = -4.88 \text{ ppm}$).

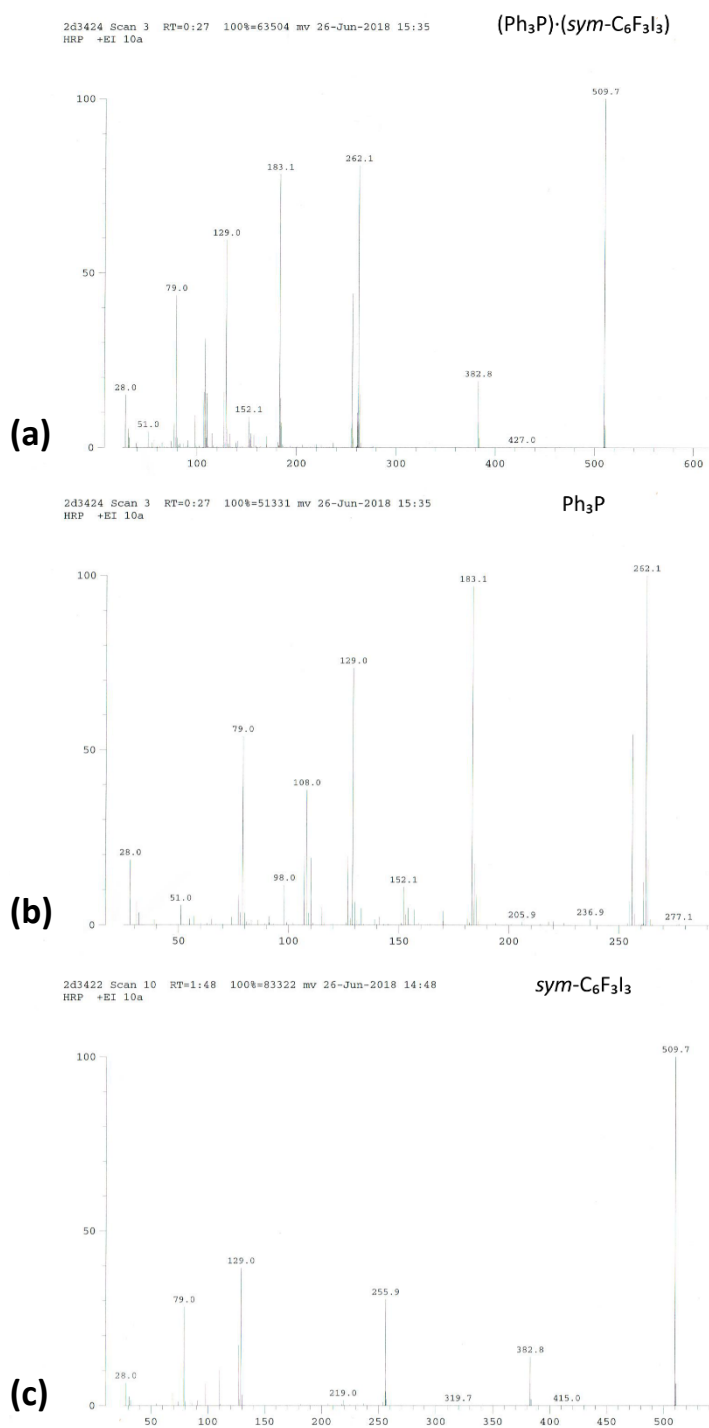


Figure S7. Electron impact mass spectra obtained for pure cocrystal **1** (a), Ph₃P (b) and sym-C₆F₃I₃ (c) from the Kratos Concept Mass Spectrometer at University of Ottawa. No peak corresponding to the cocrystal was observed.

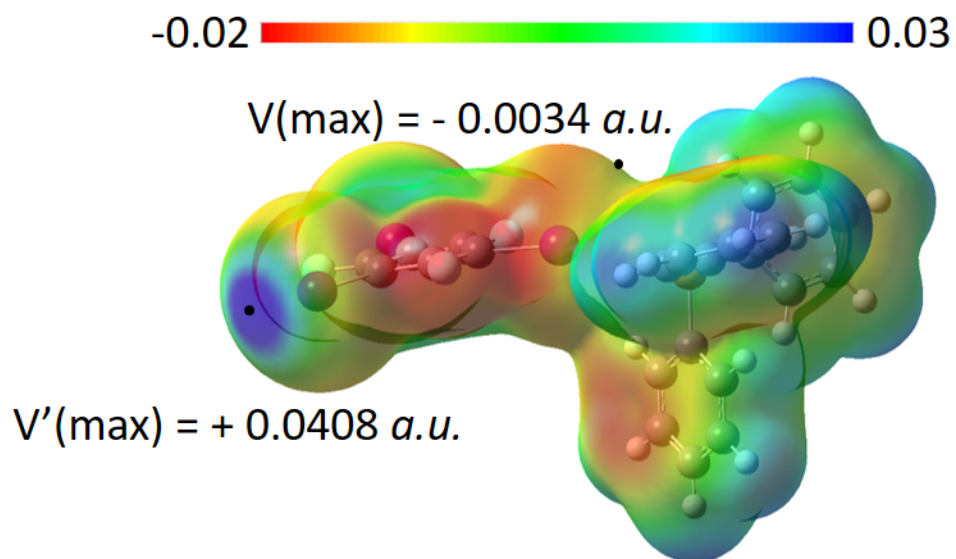


Figure S8. Electrostatic potential (ESP) map of cocrystal **1** on the 0.001 electrons bohr⁻³ molecular surface. Blue and red depict the largest (positive) and negative potentials, respectively. The corresponding scale is shown on the top. The $V'(\text{max})$ value of the obscured iodine atom at back is 0.0406 *a.u.*

Table S1. Crystallographic Data and Selected Data Collection Parameters for Halogen-Bonded Cocrystals

	1	2
Empirical Formula	C ₂₄ H ₁₅ F ₃ I ₃ P	C ₂₄ H ₁₅ F ₃ I ₃ OP
Formula Weight	772.03	788.03
Crystal Size, mm ³	0.460 × 0.320 × 0.190	0.900 × 0.320 × 0.190
Crystal System	Triclinic	Monoclinic
Space Group	<i>P</i> $\bar{1}$	<i>P</i> 2 ₁ / <i>C</i>
<i>Z</i>	2	4
Volume, Å ³	1258.6 (2)	2469.7 (6)
Calculated density, Mg m ⁻³	2.037	2.119
<i>a</i> , Å	9.1640 (9)	14.230 (2)
<i>b</i> , Å	10.9788 (11)	10.1079 (14)
<i>c</i> , Å	13.5101 (13)	17.790 (2)
α , deg	87.9470 (10)	90
β , deg	72.5210 (10)	105.164 (2)
γ , deg	76.2900 (10)	90
Absorption coefficient, mm ⁻¹	3.820	3.899
<i>F</i> (000)	720	1472
θ range for data collection, °	1.571 to 28.201	2.338 to 30.459
Limiting indices	-12 ≤ <i>h</i> ≤ 12, -14 ≤ <i>k</i> ≤ 14, -17 ≤ <i>l</i> ≤ 17	-19 ≤ <i>h</i> ≤ 19, -13 ≤ <i>k</i> ≤ 13, -23 ≤ <i>l</i> ≤ 24
Reflections collected/ unique	21984 / 5727	29024 / 6464
<i>R</i> _{int}	0.0214	0.0291
Completeness to $\theta = 25.242^\circ$, %	99.9	100.0
Max and min transmission	0.746 and 0.581	0.746 and 0.504
Data/ restraints/ parameters	5727 / 0 / 280	6464 / 0 / 289
Goodness-of-fit on <i>F</i> ²	1.026	1.012
Final <i>R</i> indices [<i>I</i> > 2 σ (<i>I</i>)]	<i>R</i> ₁ = 0.0281, <i>wR</i> ₂ = 0.0568	<i>R</i> ₁ = 0.0264, <i>wR</i> ₂ = 0.0573
<i>R</i> indices (all data)	<i>R</i> ₁ = 0.0373, <i>wR</i> ₂ = 0.0607	<i>R</i> ₁ = 0.0386, <i>wR</i> ₂ = 0.0624
largest diff. peak and hole, e ⁻ Å ⁻³	1.166 and -1.017	0.814 and -1.071

Table S2. CSD Entries Featuring Phosphorus-Halogen Non-Covalent Contacts Shorter Than the Sum of Their van der Waals' Radii (but significantly longer than the sum of their covalent radii)^a

	compound	CCDC entry	XB donor
self	3,5,7,9-Tetra-t-butyl-4,4-di-iodo-4-sila-1,2,6,8,10,11-hexaphosphapentacyclo(4.3.2.0 ^{2,5} .0 ^{3,10} .0 ^{7,11})undec-8-ene	DOQQOP	I
	((8-iodo-1-naphthyl)methyl)(phenyl)phosphine	EGOVOM	I
	(η^2 -1,2-bis(diphenylphosphino)ethyne)-carbonyl-(hydridotris(3,4,5-trimethylpyrazol-1-yl)borate)-iodotungsten(iii) hexafluorophosphate dichloromethane solvate	HAXYIR	I
	1,3-bis(Iodo)-2,4-bis(tri-t-butylsilyl)tetraphosphetane	HOVHUW	I
	3,6,8,10-Tetra-t-butyl-1,4-di-iodo-1,2,4,5,7,9-hexaphosphahexacyclo(4.4.0.02,5.03,9.04,8.07,10)decane	HUKBUL	I
	bis(7-iodo-2,3-dihydrothieno[3,4-b][1,4]dioxin-5-yl)(phenyl)phosphine	XIZCEQ	I
	tris(2-Bromo-5-thienyl)phosphine	COJWUU	Br
	1-Bromo-8-(diethoxyphosphino)naphthalene	OJEJET	Br
	1,8-bis(Dichlorophosphino)naphthalene	GUTJEK	Cl
	(C ₁₄ H ₁₀ Ag Mo ₂ O ₄ P ₆ ⁺) _n , n(C H ₂ Cl ₂), n(C ₁₆ Al F ₃₆ O ₄ ⁻)	LUJKOR	Cl
	6,6,7,7-Tetrachloro-2,4-dimethyl-2,4-diaza-1,5-diphosphabicyclo(3.1.1)heptan-3-one	XOMMOB	Cl
cocrystal	1-Diphenylphosphino-2-methyl-1,2-dicarbadodecaborane(10) hemikis(iodine)	ECISIT	I
solvate	(E)-1-(2,4-dinitrophenyl)-2-(2-(diphenylphosphino)benzylidene)hydrazine chloroform solvate	BUWXUO	Cl
	hexakis(μ -phosphido)-pentakis(η^5 -cyclopentadienyl)-penta-molybdenum dichloromethane solvate	HAHHAC	Cl
	1,4-(Biphenyl-2,2'-diyl)-2,3-diethyl-1,1,4,4-tetraphenyl-1,2,3,4-tetraphosphy-[4]catenium hemikis(hexachloro-tin) pentachloro-tin chloroform solvate	NIDREY	Cl

a. For a survey of phosphines interacting with molecular iodine at much shorter distances, see also W. T. Pennington, T. W. Hanks, and H. D. Arman (2007) *Halogen Bonding with Dihalogens and Interhalogens*. In: Metrangolo P., Resnati G. (eds) *Halogen Bonding. Structure and Bonding*, vol 126, pp65-104, Springer, Berlin, Heidelberg.

References

1. M. J. Frisch, G. W. Trucks, H. B. Schlegel, G. E. Scuseria, M. A. Robb, J. R. Cheeseman, G. Scalmani, V. Barone, B. Mennucci et al. Gaussian 09, Revision D. 01; Gaussian Inc., Wallingford, CT, 2013
2. R. Dennington, T. Keith, J. Milliam, GaussView, Version 4.1; Semichem Inc., Shawnee Mission, KS, 2007
3. APEX 2, Bruker AXS Inc., Madison, Wisconsin, USA, 2012.
4. G. M. Sheldrick, SADABS, Program for empirical X-ray absorption correction, Bruker AXS Inc., Madison, Wisconsin, USA, 2004.
5. G. M. Sheldrick, *Acta Crystallogr. C*, 2015, **71**, 3–8.
6. L. J. Farrugia, *J. Appl. Crystallogr.*, 1999, **32**, 837–838.